Proc. Natl. Acad. Sci. USA
Vol. 93, pp. 8005–8010, July 1996
Neurobiology

GABAergic feedforward projections from the inferior colliculus to the medial geniculate body

JEFFERY A. WINER*†, RICHARD L. SAINT MARIE‡, DAVID T. LARUE*, AND DOUGLAS L. OLIVER§

*Division of Neurobiology, Department of Molecular and Cell Biology, University of California at Berkeley, Berkeley, CA 94720-3200; ‡Department of Neuroanatomy, The House Ear Institute, 2100 West Third Street, Los Angeles, CA 90057; and §Department of Anatomy, The University of Connecticut Health Center, Farmington, CT 06030-3405

Communicated by Carla J. Shatz, University of California, Berkeley, CA, February 21, 1996 (received for review November 27, 1995)

ABSTRACT **A novel and robust projection from γ-aminobutyric acid-containing (GABAergic) inferior colliculus neurons to the medial geniculate body (MGB) was discovered in the cat using axoplasmic transport methods combined with immunocytochemistry. This input travels with the classical inferior colliculus projection to the MGB, and it is a direct ascending GABAergic pathway to the sensory thalamus that may be inhibitory. This bilateral projection constitutes 10–30% of the neurons in the auditory tectothalamic system. Studies by others have shown that comparable input to the corresponding thalamic visual or somesthetic nuclei is absent. This suggests that monosynaptic inhibition or disinhibition is a prominent feature in the MGB and that differences in neural circuitry distinguish it from its thalamic visual and somesthetic counterparts.**

The thalamus is the gateway controlling the flow of sensory information reaching the cerebral cortex (1). The consensus is that input ascending to the primary thalamic nuclei for hearing (2), vision (3), and somesthesis (4) is entirely excitatory. We describe here a prominent and unexpected projection from γ-aminobutyric acid-containing (GABAergic) cells in the inferior colliculus (IC) to the medial geniculate body (MGB) in the auditory tectothalamic (TT) pathway that constitutes an exception to this principle. This suggests that there is a convergence of classical excitatory and putatively inhibitory projections within the MGB and that an ascending pathway considered as neurochemically unitary in fact contains more than one channel. This striking difference in feedforward input between the auditory thalamus and other thalamic sensory nuclei is surprising since each has similar structural and intrinsic features (5–7), shared physiological properties (8–10), analogous cortical projection patterns (11–13), and a closely related neurochemical organization (14, 15). The present results suggest that, despite these parallels, there must be differences in circuitry and information processing regimes within the sensory thalamus.

METHODS

We injected either of two axonally transported tracers, wheat germ agglutinin apo-horseradish peroxidase gold (WAHG) or horseradish peroxidase, in MGB nuclei in adult cats to label the projection neurons. Each tracer is incorporated into axon terminals and accumulates in the cytoplasm of the cells of origin (16, 17). GABA was then localized immunocytochemically within the somata of the retrogradely labeled neurons.

WAHG contains wheat germ agglutinin conjugated to enzymatically inactivated horseradish peroxidase coupled to colloidal gold (E·Y Laboratories, San Mateo, CA). It was injected by pressure into the MGB of an adult cat anesthetized with isoflurane at a level that suppressed all nociceptive reflexes. All experimental procedures followed the applicable and approved institutional animal care and use protocols. Four unilateral penetrations were made using stereotaxic coordinates to target specific nuclei in various subdivisions. A total of seven, 50-nl deposits were made at 500-μm intervals along a track with a glass micropipet; the net volume was ~1.5 μl.

The animal was reanesthetized 3 days later and perfused with PBS followed by 2% paraformaldehyde and 3% glutaraldehyde in 0.12 M PB. Vibratome sections, 50-μm-thick, were collected in 0.1 M PB and placed in blocking serum (5% normal goat serum) for 60 min. Tissue was incubated overnight at 4°C in rabbit-anti-GABA (Incstar, Stillwater, MN) diluted 1:5000 and then reacted using avidin-biotin immunoperoxidase (Vectastain, Vector Laboratories, Burlingame, CA) with diaminobenzidine as the chromagen. WAHG labeling was intensified with silver (IntenSE-M, Amersham) for light microscopy.

Retrogradely labeled (WAHG-positive) and double-labeled (WAHG- and GABA-positive) midbrain cells were plotted at five caudorostral levels on an X-Y recorder coupled to the microscope stage. Only neurons in the most superficial 1–2 μm were analyzed since the glutaraldehyde fixation impeded deeper penetration of the immunoreagents. Neurons were plotted and counted when they contained granules of retrogradely transported material in the same superficial focal plane as the GABA immunostaining. Double-labeled cells were unambiguously GABA-positive and contained abundant black WAHG/silver granules.

Horseradish peroxidase (type VI, 10–20%; Sigma) was pressure injected unilaterally in four cats anesthetized with ketamine, xylazine, and pentobarbital. Each cat received three to six injections at multiple sites with a total volume of 1.0–4.0 μl/case. After 2–3 days, animals were reanesthetized and perfused with 50–100 ml of PB (0.12 M, pH 7.4) with 2% sucrose, 0.05% lidocaine, and 0.004% $CaCl_2$, then 500 ml of buffered 0.5% paraformaldehyde and 1% glutaraldehyde, and then 1000 ml of buffered 1% paraformaldehyde and 3%

The publication costs of this article were defrayed in part by page charge payment. This article must therefore be hereby marked "*advertisement*" in accordance with 18 U.S.C. §1734 solely to indicate this fact.

Abbreviations: GABAergic, γ-aminobutyric acid-containing; HRP, horseradish peroxidase; IC, inferior colliculus; MGB, medial geniculate body; TT, tectothalamic pathway; WAHG, wheat germ agglutinin apo-horseradish peroxidase gold; APt, anterior pretectum; Aq, cerebral aqueduct; BIC, brachium of the inferior colliculus; CG, central gray; CN, central nucleus; CP, cerebral peduncle; D, dorsal nucleus or dorsal; DC, dorsal cortex of the inferior colliculus or dorsal caudal nucleus of the medial geniculate body; DD, deep dorsal nucleus; DS, dorsal superficial nucleus; EW, Edinger–Westphal nucleus; GABA, γ-aminobutyric acid; L, lateral; LGB, lateral geniculate body; LMN, lateral mesencephalic nucleus; LN, lateral nucleus; LP, lateral posterior nucleus; M, medial division or medial; MRF, mesencephalic reticular formation; OR, optic radiations; OT, optic tract; Ov, pars ovoidea; Pt, pretectum; Pul, pulvinar; Ret, thalamic reticular nucleus; RN, red nucleus; RP, rostral pole nucleus; SC, superior colliculus; Sg, suprageniculate nucleus; Spf, subparafasicular nucleus; SpN, suprapeduncular nucleus; V, ventral nucleus or ventral; Vb, ventrobasal complex; III, oculomotor nerve.

†To whom reprint requests should be addressed. e-mail: jaw@uclink4.berkeley.edu.

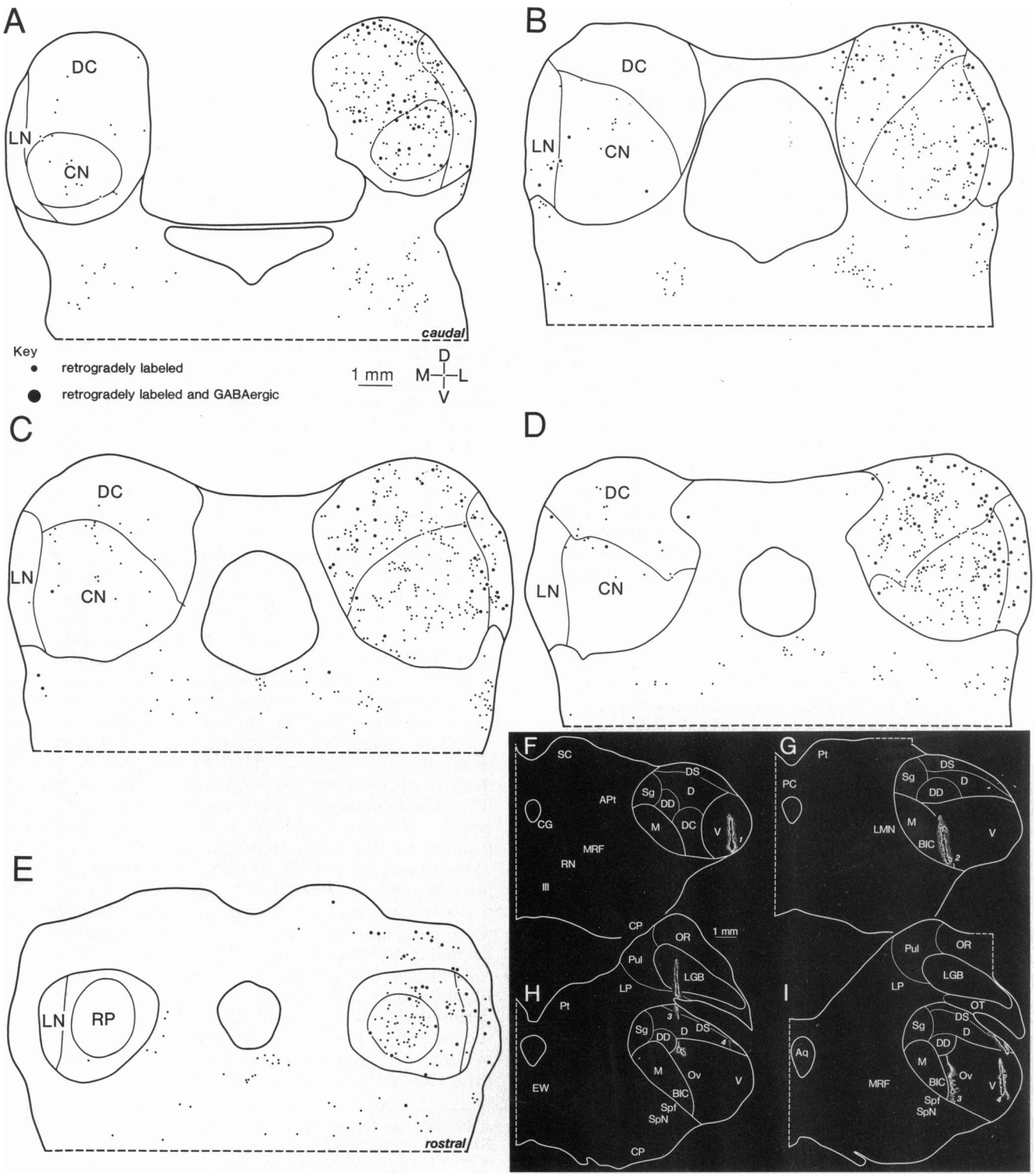

FIG. 1. (*A–E*) Plots of the distribution of retrogradely (single) labeled neurons (small dots) and of retrogradely marked and γ-aminobutyric acidergic (double-labeled) cells (large dots) in IC subdivisions in transverse sections after WAHG injections in the MGB. A dot represents one neuron. Each IC section is 600 μm from its neighbor. Characteristic labeled neurons appear in Fig. 2. (*F–I*) The WAHG injection sites in the MGB. The center of each track (black) is surrounded by the diffusion zone (stippled), which represents the effective uptake site. The deposits (*1–4*) targeted the MGB 25% in front of its caudal pole (*F*) and 25% behind its rostral pole (*I*).

glutaraldehyde (18). Brains were blocked and Vibratome-sectioned at 60 μm. Every third section was collected in 0.12 M PB, and the horseradish peroxidase was visualized with heavy metal-intensified diaminobenzidine (19). Sections were transferred to a blocking solution containing 1.5% normal sheep serum in PBS, and then incubated overnight at room temperature with double-affinity purified rabbit-anti-GABA (20) in PBS (dilution: 1:8,000–1:16,000). Antibody binding was visualized using rabbit avidin-biotin immunoperoxidase (Vector Laboratories) with unintensified diaminobenzidine.

Retrogradely labeled and double-labeled neurons were identified at 750× and plotted at four to seven caudorostral levels at 30× with a drawing tube. Cell counts were made from these plots.

Table 1. Proportion of GABAergic projection neurons in inferior colliculus subdivisions after injection of retrograde tracers in the medial geniculate body.

Experiment and tracer	Injection site	Inferior colliculus subdivision: Central nucleus — Number of retrogradely labeled cells	Central nucleus — Percentage of retrogradely labeled, GABA-positive neurons	Dorsal cortex — Number of retrogradely labeled cells	Dorsal cortex — Percentage of retrogradely labeled, GABA-positive neurons	Lateral nucleus — Number of retrogradely labeled cells	Lateral nucleus — Percentage of retrogradely labeled, GABA-positive neurons	Mean percentage double labeled
Ipsilateral								
1. WAHG	Ventral, dorsal, and medial divisions	433	14	429	21	96	35	19
2. HRP	Dorsal and medial divisions	146	21	38	26	24	25	22
3. HRP	Dorsal and medial divisions	71	17	29	48	11	27	26
4. HRP	Ventral, dorsal, and medial divisions	163	14	30	27	10	50	18
5. HRP	Ventral and dorsal divisions	25	36	89	18	27	15	21
Mean ± standard deviation			20 ± 9		28 ± 12		30 ± 13	21 ± 3
Contralateral								
1. WAHG	Ventral, dorsal, and medial divisions	53	9	26	4	8	38	10

RESULTS

Injection Sites. We present only one experiment in detail since the results were similar in each of the five cases and with both tracers (Table 1, experiment 1). Three of the four WAHG deposits involved the ventral division, where the lateral, low frequency (Fig. 1 *F:1* and *I:4*) and the medial, high frequency (Fig. 1*I:3*) representations of the tonotopic sequence were targeted (21). The medial division (Fig. 1*G:2*) and the dorsal division (Fig. 1 *H:3* and *I*, upper part of *4*) were also injected. The deposits were confined to the MGB except for minor involvement of the lateral geniculate body; this cannot account for the present results since there is no projection from the IC to the lateral geniculate body (22).

Patterns of Retrograde Labeling. Several thousand IC neurons were labeled (Fig. 1 *A-E*). Representative sections at intervals equidistant from the caudal (Fig. 1*A*) to the rostral (Fig. 1*E*) IC are shown; the pattern was similar in the intervening material. Among the retrogradely labeled neurons (Fig. 1 *A-E*, small dots), nearly 20% colocalized GABA and WAHG (Fig. 1 *A-E*, large dots) ipsilaterally and were classified as double-labeled (Table 1). Such neurons had many black granules of silver-intensified colloidal gold in their cytoplasm and were strongly immunopositive (Fig. 2 *A-C*); they were differentiated readily from neurons that were either labeled only retrogradely (Fig. 2*D*) or were only immunopositive (not shown). The neuropil and glial cells were entirely devoid of these particles.

Distribution of Double-Labeled Neurons. GABAergic TT neurons were found bilaterally, but the ipsilateral neurons represented more than 90% of the total. This proportion matched the results in previous connectional studies (23). The ipsilateral projection neurons were distributed through the dorsolateral-to-ventromedial extent of the IC; this suggests that the tracer deposits probably spanned much of the topographic representation of frequency in each MGB division (24–26). Single- and double-labeled neurons were also found in the lateral tegmental region of the midbrain (27).

Proportions and Structure of Double-Labeled Neurons. GABAergic projection neurons were always found in every IC subdivision, interspersed with immunonegative TT cells. Double-labeled neurons were most common in the dorsal cortex and lateral (external) nucleus, averaging 28 and 30%, respec-

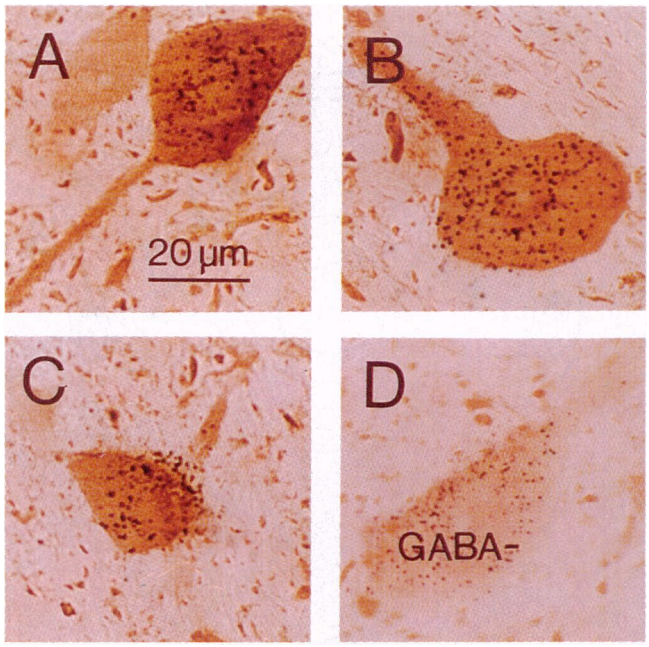

FIG. 2. Examples of single- and double-labeled neurons in IC subdivisions after WAHG deposits (see Fig. 1 *F–I*) in the ipsilateral MGB. The silver-intensified WAHG particles were black and less than 0.5 μm in diameter, and the GABA immunostaining was dark golden-brown. (*A*) A double-labeled central nucleus cell; the WAHG grains were confined entirely to the cytoplasm; (*B*) from the dorsal cortex; (*C*) from the lateral nucleus; (*D*) a WAHG-labeled, GABA-negative, lateral nucleus neuron. Planachromat, numerical aperture, 0.7, × 660.

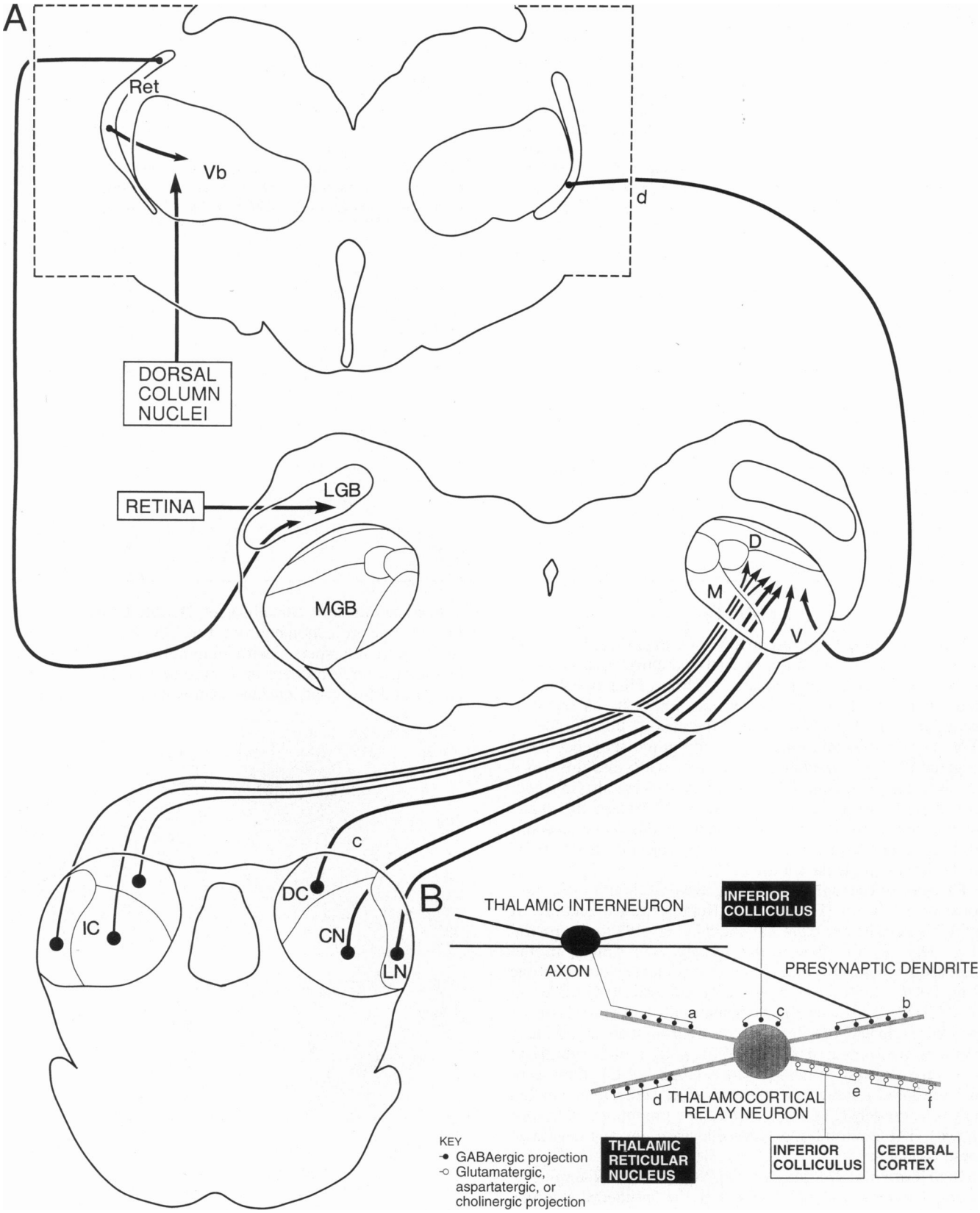

FIG. 3. Summary of results. (*A*) Origins (circles) and targets (arrowheads) of extrinsic input to the main sensory thalamic nuclei (47). The projections shown are GABAergic except those from the retina and dorsal column nuclei (large arrowheads). *c* and *d*, GABAergic input from the inferior colliculus (*c*) and thalamic reticular nucleus (*d*), respectively. (*B*) Synthesis of synaptic organization in the ventral division of the medial geniculate body. The postsynaptic target(s) of GABAergic TT axons are unknown. Immunocytochemical evidence from postembedded material shows that principal cell perikarya receive six times more GABAergic axosomatic puncta than do GABAergic cells (48). While the evidence that the GABAergic TT neurons are the source of this input is indirect, the predominantly axo- and dendrodendritic distribution of GABAergic synapses from intrinsic (44, 45) and extrinsic (14, 49) sources suggests that the perikaryon is not the principal target; this is shown schematically (*c*) since it has not been demonstrated at the ultrastructural level. Modified from ref. 50.

tively, of the TT cells in these regions; the central nucleus had fewer, about 20%. Overall, 21% of the TT neurons were GABA-immunoreactive (range, 18–26%; Table 1). There was a wide range in size and shape among double-labeled neuronal somata, which included medium sized, spindle-shaped cells (Fig. 2*C*), and the largest IC neurons, up to 33 μm in average somatic diameter (Fig. 2*B*). This variability matched the distribution reported for GABAergic cells in the central nucleus (28).

DISCUSSION

This is the first demonstration of a GABAergic TT pathway (29, 30), and it has implications for information processing in the auditory thalamus. We consider below the parallels between excitatory and inhibitory tectothalamic projections, comment on differences between the MGB and other thalamic sensory nuclei, and conclude with a speculation on the function of ascending GABAergic input in the larger context of thalamic substrates for inhibition.

The GABAergic TT projection ascends with the classical, presumably excitatory, input (2, 22) to the auditory thalamus (Fig. 3*A*) via the brachium of the inferior colliculus. Both pathways arise from all IC subdivisions, including an exclusively auditory component (central nucleus), input from multimodal IC regions (dorsal cortex; lateral nucleus), and extracollicular midbrain projections (tegmentum; sagulum) (22). Ascending, inhibitory projections may be common to all parts of the IC and to related parts of the midbrain. Two other implications follow from these observations. First, the high proportion of double-labeled cells suggests that surprisingly few IC GABAergic neurons have projections confined to the inferior colliculus. Perhaps the definition of a local circuit neuron should be enlarged to include GABAergic cells with both intrinsic and remote projections. A second conclusion is that the feedforward inhibition so prevalent in the auditory brain stem (31–33) is also found in the TT pathway.

Feedforward inhibition to the visual thalamus is limited, and in the somesthetic thalamus it is virtually nonexistent. Except for a few GABAergic retinal ganglion cells in rodents (34), almost all ganglion cells and their axons are nonGABAergic (35, 36). While they are not generally regarded as part of the primary pathway, the pretectal nuclei provide a significant GABAergic projection to the visual thalamus; this input is thought to inhibit local GABAergic thalamic neurons, thus disinhibiting thalamocortical cells (37). GABAergic neurons are plentiful in the dorsal column nuclei, although none or few are presynaptic to neurons in thalamic somesthetic nuclei (38). This suggests that feedforward inhibition in the thalamic nuclei may be modality-specific (Fig. 3*A*).

There is little physiological evidence available as to the functions that a putatively inhibitory ascending input to the MGB might serve. The largest GABAergic TT cells could convey monosynaptic inhibition rapidly to thalamocortical relay cells (Fig. 3*B:c*). Such a projection might elicit inhibitory postsynaptic effects in the auditory thalamus prior to the influence of excitatory input. The smaller GABAergic TT cells presumably have slower conduction velocities, and consequently their postsynaptic effects would be expected to occur later. Among the candidate processes that inhibition might affect are the shaping of spectral cues (39), modulating intensity-dependent inhibition (40), enhancing selectivity for species-specific vocalizations (41), altering the spontaneous discharge of thalamocortical cells (26), or affecting the long term excitability of large populations of neurons (42). Neither the large nor the small GABAergic TT cells are involved in early coding in the temporal domain or in the establishment of binaural properties, both of which are represented robustly at prethalamic levels (43). Inhibition converging upon or arising within the thalamus may nonetheless influence these processes in ways that remain to be demonstrated.

Perhaps each of the four forms of GABAergic input to the MGB has a different and specific role. We speculate that the local axonal projections of Golgi type II cells (Fig. 3*B:a*) are well suited to enhance the coding and discharge synchrony of small ensembles of nearby thalamocortical neurons (44, 45). The dendrodendritic synapses originating from local circuit cells (Fig. 3*B:b*) are situated ideally to suppress signal propagation along principal cell distal dendrites, thus amplifying the action of synapses nearer the spike initiation zone. Thalamic reticular nucleus input (Fig. 3*B:d*) could focus attentional processes by regulating modality-specific excitability (46). Finally, the GABAergic TT pathway (Fig. 3*B:c*) might permit ascending inhibitory midbrain influences to reach MGB neurons monosynaptically and perhaps exert influence across a broad temporal spectrum.

These scenarios are inconsistent with the proposition that the auditory thalamus conveys ascending information passively to cortical or subcortical targets. GABAergic feedforward projections are a substantive and distinctive part of the classical ascending midbrain pathway to the auditory forebrain, and they may entail a unique mechanism gating the flow of collicular information through the thalamus.

We thank S. Paydar for experimental assistance. Dr. R.J. Wenthold generously contributed the antiserum. This work was supported by National Institutes of Health Grants RO1 DC02319-16 (J.A.W.), RO1 DC00189 (D.L.O.), and RO1 DC00726 (R.L.S.M.).

1. Le Gros Clark, W. E. (1932) *Brain* **55,** 406–470.
2. Hu, B., Senatorov, V. & Mooney, D. (1994) *J. Physiol. (London)* **479,** 217–231.
3. Ottersen, O. P. & Storm-Mathisen, J. (1984) *J. Comp. Neurol.* **229,** 374–386.
4. Salt, T. E. (1988) in *Cellular Thalamic Mechanisms*, eds. Bentivoglio, M. & Spreafico, R. (Excerpta Medica, Amsterdam), pp. 296–310.
5. Morest, D. K. (1964) *J. Anat. (London)* **98,** 611–630.
6. Friedlander, M. J., Lin, C.-S., Stanford, L. R. & Sherman, S. M. (1981) *J. Neurophysiol.* **46,** 80–129.
7. Scheibel, M. E. & Scheibel, A. B. (1966) in *The Thalamus*, eds. Purpura, D. P. & Yahr, M. D. (Columbia University Press, New York), pp. 13–46.
8. Imig, T. J. & Morel, A. (1985) *J. Neurophysiol.* **53,** 309–340.
9. Bishop, P. O., Kozak, W., Levick, W. R. & Vakkur, G. J. (1962) *J. Physiol. (London)* **163,** 503–539.
10. Mountcastle, V. B. & Henneman, E. (1949) *J. Neurophysiol.* **12,** 85–100.
11. Niimi, K. & Matsuoka, H. (1979) *Adv. Anat. Embryol. Cell Biol.* **57,** 1–56.
12. Geisert, E. E., Jr. (1980) *J. Comp. Neurol.* **190,** 793–812.
13. Spreafico, R., Hayes, N. L. & Rustioni, A. (1981) *J. Comp. Neurol.* **203,** 67–90.
14. Jones, E. G. (1985) *The Thalamus* (Plenum Press, New York), pp. 815, 153–223.
15. Aitkin, L. M. (1989) in *Handbook of Chemical Neuroanatomy, Integrated Systems of the CNS, Central Visual, Auditory, Somatosensory, Gustatory*, eds. Björklund, A., Hökfelt, T. & Swanson, L. W. (Elsevier, Amsterdam), Vol. 4, Part I, pp. 165–218.
16. Basbaum, A. I. & Menetrey, D. (1987) *J. Comp. Neurol.* **261,** 306–318.
17. Mesulam, M.-M. (1982) in *Tracing Neural Connections with Horseradish Peroxidase*, ed. Mesulam, M.-M. (John Wiley & Sons, Chichester, England), pp. 1–152.
18. Saint Marie, R. L., Ostapoff, E.-M., Morest, D. K. & Wenthold, R. J. (1989) *J. Comp. Neurol.* **279,** 382–396.
19. Adams, J. C. (1981) *J. Histochem. Cytochem.* **29,** 775.
20. Wenthold, R. J., Huie, E., Altschuler, R. A. & Reeks, K. A. (1987) *Neuroscience* **22,** 897–912.
21. Aitkin, L. M. & Webster, W. R. (1972) *J. Neurophysiol.* **35,** 365–380.

22. Aitkin, L. M. (1986) *The Auditory Midbrain. Structure and Function in the Central Auditory Pathway* (Humana Press, Clifton, NJ), pp. 75–100.
23. Calford, M. B. & Aitkin, L. M. (1983) *J. Neurosci.* **3,** 2365–2380.
24. Merzenich, M. M. & Reid, M. D. (1974) *Brain Res.* **77,** 397–415.
25. Winer, J. A. (1992) in *The Mammalian Auditory Pathway: Neuroanatomy, Springer Handbook of Auditory Research*, eds. Webster, D. B., Popper, A. N. & Fay, R. R. (Springer-Verlag, New York), Vol. 1, pp. 222–409.
26. Clarey, J. C., Barone, P. & Imig, T. J. (1992) in *The Mammalian Auditory Pathway: Neurophysiology, Springer Handbook of Auditory Research*, eds. Popper, A. N. & Fay, R. R. (Springer-Verlag, New York), Vol. 2, pp. 232–334.
27. Henkel, C. K. (1983) *Brain Res.* **259,** 21–30.
28. Oliver, D. L., Winer, J. A., Beckius, G. E. & Saint Marie, R. L. (1994) *J. Comp. Neurol.* **340,** 27–42.
29. Hutson, K. A., Glendenning, K. K., Baker, B. N. & Masterton, R. B. (1993) *Proc. Soc. Neurosci.* **19,** 1203 (abstr.).
30. Paydar, S., Saint Marie, R. L., Oliver, D. L., Larue, D. T. & Winer, J. A. (1994) *Proc. Soc. Neurosci.* **20,** 976 (abstr.).
31. Saint Marie, R. L., Benson, C. G., Ostapoff, E.-M., & Morest, D. K. (1991) *Hearing Res.* **51,** 11–28.
32. Oliver, D. L. & Huerta, M. F. (1992) in *The Mammalian Auditory Pathway: Neuroanatomy, Springer Handbook of Auditory Research*, eds. Webster, D. B., Popper, A. N. & Fay, R. R. (Springer-Verlag, New York), Vol. 1, pp. 168–221.
33. Winer, J. A., Larue, D. T. & Pollak, G. D. (1995) *J. Comp. Neurol.* **355,** 317–353.
34. Lugo-Garcia, N. & Blanco, H. (1991) *Brain Res.* **564,** 19–26.
35. Boos, R., Müller, F. & Wässle, H. (1990) *J. Neurophysiol.* **64,** 1368–1379.
36. Montero, V. M. (1990) *Vis. Neurosci.* **4,** 437–443.
37. Cucchiaro, J. B., Bickford, M. E. & Sherman, S. M. (1991) *Neuroscience* **41,** 213–226.
38. De Biasi, S. & Rustioni, A. (1990) *J. Histochem. Cytochem.* **38,** 1745–1754.
39. Imig, T. J., Poirier, P. & Samson, F. K. (1994) *Proc. Soc. Neurosci.* **20,** 322 (abstr.).
40. Ivarsson, C., de Ribaupierre, Y. & de Ribaupierre, F. (1988) *J. Neurophysiol.* **59,** 586–606.
41. Olsen, J. F. & Rauschecker, J. P. (1992) *Proc. Soc. Neurosci.* **18,** 883 (abstr.).
42. Aitkin, L. M. & Dunlop, C. W. (1969) *Exp. Brain Res.* **7,** 68–83.
43. Irvine, D. R. F. (1992) in *The Mammalian Auditory Pathway: Neurophysiology, Springer Handbook of Auditory Research,* eds. Popper, A. N. & Fay, R. R. (Springer-Verlag, New York), Vol. 2, pp. 153–231.
44. Morest, D. K. (1971) *Z. Anat. Entwicklungsgesch.* **133,** 216–246.
45. Morest, D. K. (1975) *J. Comp. Neurol.* **162,** 157–194.
46. Crick, F. (1984) *Proc. Natl. Acad. Sci. USA* **81,** 4586–4590.
47. Winer, J. A. & Morest, D. K. (1983) *J. Neurosci.* **3,** 2629–2651.
48. Winer, J. A., Khurana, S. K., Prieto, J. J. & Larue, D. T. (1993) *Proc. Soc. Neurosci.* **19,** 1426 (abstr.).
49. Montero, V. M. (1983) *Exp. Brain Res.* **51,** 338–342.
50. Winer, J. A. & Larue, D. T. (1996) *Proc. Natl. Acad. Sci. USA* **93,** 3083–3087.